European Journal of Chemistry

View Journal Online
View Article Online

Experimental comparison of electrochemical and quantum transport-based biodetection methods for RNA cancer biomarkers

Ajoke Williams [1], Keshani Gayathri Gunasinghe Pattiya Arachchillage [1], Subrata Chandra [1], and Juan Manuel Artés Vivancos [1,2,*]

[1] *Department of Chemistry, University of Massachusetts Lowell, Lowell MA, 01854, United States*
[2] *European Research Council Executive Agency, Covent Garden, Brussels, B-1049, Belgium*

* *Corresponding author at: Department of Chemistry, University of Massachusetts Lowell, Lowell MA, 01854, United States.*
e-mail: juan.artes-vivancos@ec.europa.eu (J.M. Artés Vivancos).

RESEARCH ARTICLE

10.5155/eurjchem.17.2.89-98.2748

Received: 22 December 2025
Received in revised form: 17 March 2026
Accepted: 10 April 2026
Published online: 30 June 2026
Printed: 30 June 2026

KEYWORDS

KRAS G12V
Single molecule
Bioelectrochemistry
RNA cancer biomarkers
Biomolecular electronics
Electrochemical biosensors
Molecular electronics detection

ABSTRACT

Cancer remains a leading cause of death worldwide and early-stage detection is essential to improve patient outcomes. Recent advances in nanoscale sensing have opened up new pathways for ultrasensitive, label-free detection of nucleic acid biomarkers. In this work, we compare two sensor platforms for a KRAS G12V RNA biomarker: (i) a classical bioelectrochemical sensor that exploits the redox activity of methylene blue modified DNA probes, and (ii) a recently reported quantum transport-based single-molecule sensor that measures conductance changes of individual DNA: RNA hybrids using scanning -tunneling-microscopy break-junctions (STM-BJ). By comparing both approaches, we evaluate their key performance metrics -limit of detection, specificity, and robustness- in biologically relevant complex media. The electrochemical sensor reaches a femtomolar detection limit, but fails to discriminate a single-base mismatch under the tested conditions. In contrast, the STM-BJ platform delivers attomolar sensitivity and single-base resolution; however, its operation is hindered in complex media, particularly in protein-rich environments. However, this weakness is also shared with the electrochemical approach. Our comparative analysis highlights the complementary strengths of these platforms, suggesting that integrating both could improve point-of-care cancer screening by combining sensitivity, specificity, and robustness in complex samples.

Cite this: *Eur. J. Chem.* **2026**, *17(2)*, 89-98 **Journal website**: www.eurjchem.com

1. Introduction

Cancer is a complex, multifactorial disease [1,2]. It is a devastating disease that accounts for nearly one in six deaths worldwide, corresponding to 9.7 million deaths in 2022 [3,4]. Detecting cancer early is vital, as mortality rates rise dramatically when found at advanced stages [5-7]. This underscores the necessity for rapid and sensitive biosensing technologies to implement liquid biopsy diagnostics. New highly sensitive electrical biosensors could simplify disease detection and increase survival rates [8]. In several fields such as liquid biopsy, biochemistry, and life sciences in general, the accurate detection of specific nucleic acid sequences plays a crucial role [9]. Among the various methods available, electrical nucleic acid hybridization biosensors are promising platforms [8,10-14]. These include direct electrical single-molecule detection [8,12,13,15-19] and more established electrochemical biosensors, with plenty of examples in the literature [20,21]. The former method is emerging as an ultrasensitive biosensing strategy that has high potential for miniaturization, automation, and parallelization. On the contrary, the latter is an established method that has been demonstrated in many applications. This latter kind of biosensor relies on immobilizing oligonucleotides on an electrode surface and can utilize different electrochemical techniques to detect hybridization and biorecognition processes [22]. Several methods have been reported for immobilizing the single-stranded DNA (ssDNA) probe on electrode surfaces, including self-assembled methods [11,23], direct adsorption [24,25], covalent binding [26,27], nanoparticles [28,29], and affinity-based methods, such as avidin-biotin systems [9,30]. In particular, self-assembled monolayers on electrodes have emerged as an effective approach to DNA immobilization, offering advantages such as simplicity, high orientation, and versatility [9,31]. Using these strategies, electrochemical biosensors (particularly those that target nucleic acids) are powerful tools for this kind of applications [32]. However, challenges persist, such as nonspecific adsorption of proteins that can compromise sensor surfaces and the difficulty in identifying small polymorphisms in nucleic acid sequences, leading to false positives and other problems [33].

https://dx.doi.org/10.5155/eurjchem.17.2.89-98.2748

Table 1. G12V 18 nucleotide sequences used in the experiments: The DNA probe includes binding groups; for electrochemistry, we use monothiol X = thiol binder SH-(C6 spacer) and Y = 0, for STM-BJ experiments, dithiol, X = Y = thiol binder SH-(C6 spacer). The RNA targets include sequences for both perfect match and single-base mismatches; the single-base mismatch is highlighted in underlined.

KRAS G12V mutation DNA probe sequence	Perfect match RNA target sequence	KRAS (healthy) mismatched RNA target
X-5'-GGAGCTGTT GGCG TAGGC 3'-Y	5'-CCUCGACAACCGCAUCCG-3'	5'-CCUCGACCACCGCAUCCG-3'

In this paper, we compare two electrical detection methods that target a cancer RNA biomarker. We explore the more established cyclic voltammetry (CV)-based electrochemical detection method using methylene blue [10,34] and the recently proposed single-molecule direct electrical quantum transport-based detection method [12,35]. Our results show that while the bioelectrochemical approach can detect RNA hybridization down to fM levels, it lacks specificity, providing a similar signal for mutant and wild-type KRAS sequences with this CV-based configuration. In complex media, both methods are challenged and need further research and optimization to be applied for cancer screening in liquid biopsy samples.

2. Experimental

2.1. Apparatus

All electrochemical experiments were carried out in a conventional three-electrode setup using a potentiostat from Gamry instruments (Interface 1010 B) in a 25 mM phosphate buffer medium (pH = 7.4). The Au single crystal (0.78 cm^2) was the working electrode. A silver/silver chloride (Ag/AgCl, 3 M, NaCl) electrode and a coiled platinum wire served as the reference electrode and counter electrode, respectively. All potentials presented are reported with respect to the Ag/AgCl reference electrode (RE-5B BASI) [36,37].

2.2. Chemicals and reagents

Disodium hydrogen monophosphate and sodium dihydrogen phosphate were used to prepare the 25 mM phosphate buffer (pH = 7.4) with deionized water. The buffer solution was then filtered with 20 nm pore size filters (Whatman Anotop 25 plus) before being used in the experiments. Chemicals such as acetone (HPLC plus), ethyl alcohol (pure), sulfuric acid, hydrochloric acid, disodium hydrogen monophosphate, sodium dihydrogen phosphate, Methylene blue (MB), mercaptohexanol, magnesium chloride, bovine serum albumin (BSA), and calf thymus DNA were purchased from Sigma-Aldrich. All oligonucleotides were purchased from Biosynthesis, USA (Table 1) [36-38].

2.3. Sample and solution preparation

The oligonucleotides were received in powder form and were subsequently spun down before being resuspended in a (prefiltered) 25 mM phosphate buffer (pH = 7.4). All glassware and Teflon cells were cleaned with piranha solution, prepared by combining 98% sulfuric acid and 30% hydrogen peroxide in a 3:1 (v/v) ratio (CAUTION: The piranha solution is extremely corrosive and dangerous) [36,37]. Acetone (HPLC plus) and ethyl alcohol (pure) were used to clean all other parts of the electrochemical cell. 50 mM magnesium chloride, 20 μM methylene blue and 1 mM mercaptohexanol solutions were prepared using deionized water. The thiol group in the ssDNA probe was obtained in protected form, and TCEP (Tris(2-carboxyethyl) phosphine) was used to reduce the disulfide bond, resulting in a free thiol group that could be attached to the Au surface. In a wide pH range, TCEP completely and selectively reduces disulfides in less than 5 minutes at room temperature [39].

2.4. Fabrication of a self-assembled gold electrode with ssDNA probe and MCH backfilling

We used a modified protocol based on the methodology described in previously published reports for other sequences [33]. Before each experiment, the working electrode, an Au single crystal (Goodfellow), underwent electropolishing, following the procedures previously described [17]. The G12V 18nt ssDNA probe (2 μM, 50 μL) was immobilized on an electropolished Au electrode in the electrochemical cell. Subsequently, 50 μL of 50 mM magnesium chloride was added to the same cell. The entire system was then incubated overnight. After overnight incubation, 100 μL of 1 mM mercaptohexanol (MCH) was introduced into the same cell and allowed to remain for 4 hours. The magnesium chloride served as an electrolyte, while the MCH acted as a surface backfilling agent. The MCH filled the areas on the surface that were not covered by the ssDNA probe, resulting in the formation of densely packed DNA monolayers. After the 4-hour incubation, the electrode was thoroughly rinsed with filtered 25 mM phosphate buffer to eliminate any nonspecifically bound molecules. The rinsing process involved applying 200 μL of 25 mM phosphate buffer onto the Au electrode, gently pipetting the solution up and down twenty times, removing the liquid, and repeating this cycle three times to ensure thorough rinsing. The resulting electrode, with the ssDNA probe and the MCH monolayer, was then denoted the ss-MCH-Au electrode. Subsequently, the ss-MCH-Au electrode was incubated with 20 μM methylene blue (MB) for one hour for electrochemical experiments [36,37]. An approximate DNA surface coverage can be estimated by integrating the surface-confined MB redox peak in the cyclic voltammogram using $\Gamma = Q/(nFA)$. 64 With a scan rate of 100 mV/s, a two-electron MB redox process, and a 0.78 cm^2 area of the Au electrode, surface coverage can be estimated around 1.7×10^{-11} mol/cm^2, comparable to previous published results [34].

2.5. Hybridization on the Au electrode surface

The ss-MCH-Au electrode was immersed in the target ss G12V 18nt RNA solution (4 μM, 100 μL) for one hour. This represents the perfect match scenario, where the ss G12V 18-bases DNA probe and the complementary G12V 18nt RNA target form a precise match (Table 1) [37]. After the hybridization process took place, the Au electrode underwent the aforementioned washing procedure to eliminate any nonspecifically bound molecules. Following the washing step, the electrode was known as ds-MCH Au, and it was then incubated with 20 μM methylene blue (MB) for 15 minutes to investigate the electrochemical signal. This step aimed to examine the electrochemical response generated by the interaction between the DNA:RNA hybrid formed after hybridization and MB. The same experimental protocol was applied for mismatch experiments, with the only difference being the RNA target used, which was the ss wild-type 18nt RNA target (Table 1) [36]. In these mismatch experiments, a single-base mismatch occurred after the hybridization process. For the titration limit of detection (LoD) experiments, a series of dilutions of the ss G12V 18-base RNA target were prepared, ranging from zM (zeptomolar, 10^{-21} M) to 4 μM concentrations. The same experimental protocol described above was followed for these titration experiments. For complex media assays, experiments were conducted using two other mediums: BSA

medium (at concentrations of 150 pM, 150 nM and 150 μM) and calf thymus DNA medium (at a concentration of 1.5 mM). These latter experiments aimed to evaluate the performance of the electrochemical measurements in complex environments.

2.6. Electrochemical measurements and data analysis

We used cyclic voltammetry (CV) with a scan rate of 100 mV/s, unless otherwise indicated. To investigate the dependence of scan rate on the measurements, experiments were carried out at different scan rates: 50, 100, 250, and 500 mV/s and in a pH = 7.4, 25 mM phosphate buffer medium. All the CV curves presented are the average values of three measurements. The potential range scanned during the experiments ranged from 0.0 V to -0.50 V, and the current was recorded [36,37].

2.7. STM-BJ experiments in calf thymus DNA medium and BSA medium

The STM-BJ experiments were performed according to the procedure previously described [12]. Measurements were made at room temperature using a Pico-STM Molecular Imaging head with a Nanoscope IIIa controller. A 10 nA/V preamplifier was used with bias voltages ranging from 100 mV to 20 mV. STM tips were prepared from 0.25 mm gold wire as previously described [12]. Before each run, control measurements in phosphate buffer were performed to ensure the absence of contaminants. In a typical DNA:RNA hybrid experiment, a small sample volume was added to the STM cell to achieve final concentrations in the μM range. The thiol-modified DNA probes were reduced with TCEP (Tris(2-carboxyethyl) phosphine) to generate free thiols to attach to the Au tip and substrate. During the measurements, the tip was repeatedly brought into and out of contact with the substrate, forming molecular junctions, and thousands of current–distance traces were recorded under LabVIEW control. The collected traces were analyzed using another custom LabVIEW program [36,37,40] and manual refinement was applied to remove noisy curves and retain traces with clear plateaus. Typically, this resulted in 200 traces selected out of around 4000 total acquired cruves (5% selection rate). The selected curves were combined to generate semi-logarithmic conductance histograms, and a Gaussian fitting was used to determine the most probable conductance values, as previously reported [12]. Experiments were conducted in either calf-thymus DNA (1.5 mM) or BSA (150 nM) media a minimum of 3 times [37].

3 Results and discussion

3.1. Electrochemical detection of a KRAS G12V RNA cancer biomarker

We explore the application of a common electrochemical approach to detect nucleic acids [10,34,41,42] by targeting the KRAS G12V cancer RNA biomarker [42] and compare it to a recently proposed cancer biomarker single-molecule electrical conductance detection method of cancer biomarkers [12,13]. For this, we investigated the electrochemical behavior of MB on gold electrodes modified with ssDNA and dsDNA:RNA hybrids. Table 1 presents the sequences used in the experiments, which are identical to those used in previously published single-molecule detection methods [12].

Figure 1a shows a scheme of the step-by-step procedure for preparing the DNA modified electrode, based on published protocols [9]. Briefly, the Au working electrode is initially modified with a monothiol-ended single-stranded DNA probe (ssDNA) and with mercaptohexanol (MCH) as the backfilling agent. Subsequently, MB is introduced into the electrochemical cell and allowed to incubate. The RNA target can then be introduced into the cell, leading to the formation of double-stranded DNA:RNA hybrids. Ensuring optimal access and molecular orientation of probe DNA is critical in any DNA hybridization biosensor. In this context, MCH is commonly used to provide fine-tuned control for the immobilization of biomolecules as a “backfilling agent” [11]. MCH serves a dual purpose in this regard. Firstly, it aids in the removal of nonspecifically absorbed DNA from the gold surface. Second, it helps to orient the immobilized DNA. This molecular orientation enhances the potential for hybridization [10,11,42]. The positively charged MB molecule (Figure 1a), which is used as a redox marker, is attracted to the negatively charged phosphate backbone of DNA oligonucleotides [34]. On the other hand, MB molecules can be intercalated in the Guanine bases of DNA. This electrostatic and intercalating interaction both facilitates the binding of MB to oligonucleotides that become inaccessible upon target hybridization [33,43]. We incubate monothiolated ssDNA molecules with a surface filler (MCH) to make a binary mixed monolayer on top of the Au(111) electrode surface. MB molecules can be attached to the ssDNA monolayer and the changes in the electrochemical signals can be monitored. These changes in the signal arise due to the binding of MB to the DNA and the alteration of the local environment around MB. In Figure 1b, the control/blank experiment conducted on the surface of ssDNA-MCH-Au is represented by the black cyclic voltammetry (CV) curve. The red and green CVs correspond to the results of the ssDNA probe and after adding the RNA target to hybridize, respectively. Notably, a decrease in the redox current peak of MB is observed on the ds-MCH-Au electrode in comparison to that on the ss-MCH-Au electrode. This reduction in current is an indicator for monitoring DNA:RNA hybridization and is consistent with previous electrochemical approaches for DNA sensing demonstrated in the literature [11,33,44-46]. Figures 1c and 1d present the CV at varying scan rates on the ssDNA probe and DNA:RNA hybrid samples, respectively. Measurements were carried out using scan rates of 50, 100, 250, and 500 mV/s. As observed in Figures 1c and 1d, it is evident that the peak current increases with the scan rate. Additionally, Figure 1e shows the graph of oxidative peak current against scan rate 1/2 for ss-MCH-Au (red) and ds-MCH-Au (green). The two lines exhibit slopes of 7.64×10^{-6} (ss) and 2.49×10^{-6}(ds), respectively. The linear behavior of peak current with the square root of the scan rate indicates that electrochemical processes are controlled by diffusion [9,42-44], in agreement with previous reports [47,48]. In addition, Figure 1f shows a confirmation for this trend; the data appear linear in a log-log plot. The different slopes in Figure 1e may indicate differences in the flexibility of single-strand vs. double-strand oligonucleotides, in the same direction as previous studies [16].

3.2. Specificity of the electrochemistry approach for the detection of the KRAS G12V mutation

Figure 2a contains the results of detection of the G12V RNA using CV experiments. We use the complementary G12V RNA target sequence, which hybridizes with the immobilized G12V DNA probe, forming a DNA:RNA hybrid. As discussed above, this results in a decrease of the current signal upon hybridization, indicating successful detection. On the contrary, in other experiments, we use a wild-type ‘healthy’ 18nt RNA target as the target molecule, creating a single-base mismatch DNA: RNA hybrid with the G12V DNA probe. This also results in a reduction in current. Figure 2b shows the resulting CV for these mismatched DNA: RNA hybrids. By doing so, we challenge the ability of the biosensor to discriminate between the G12V cancer biomarker and the wild-type KRAS RNA sequence (virtually present in any sample of human origin).

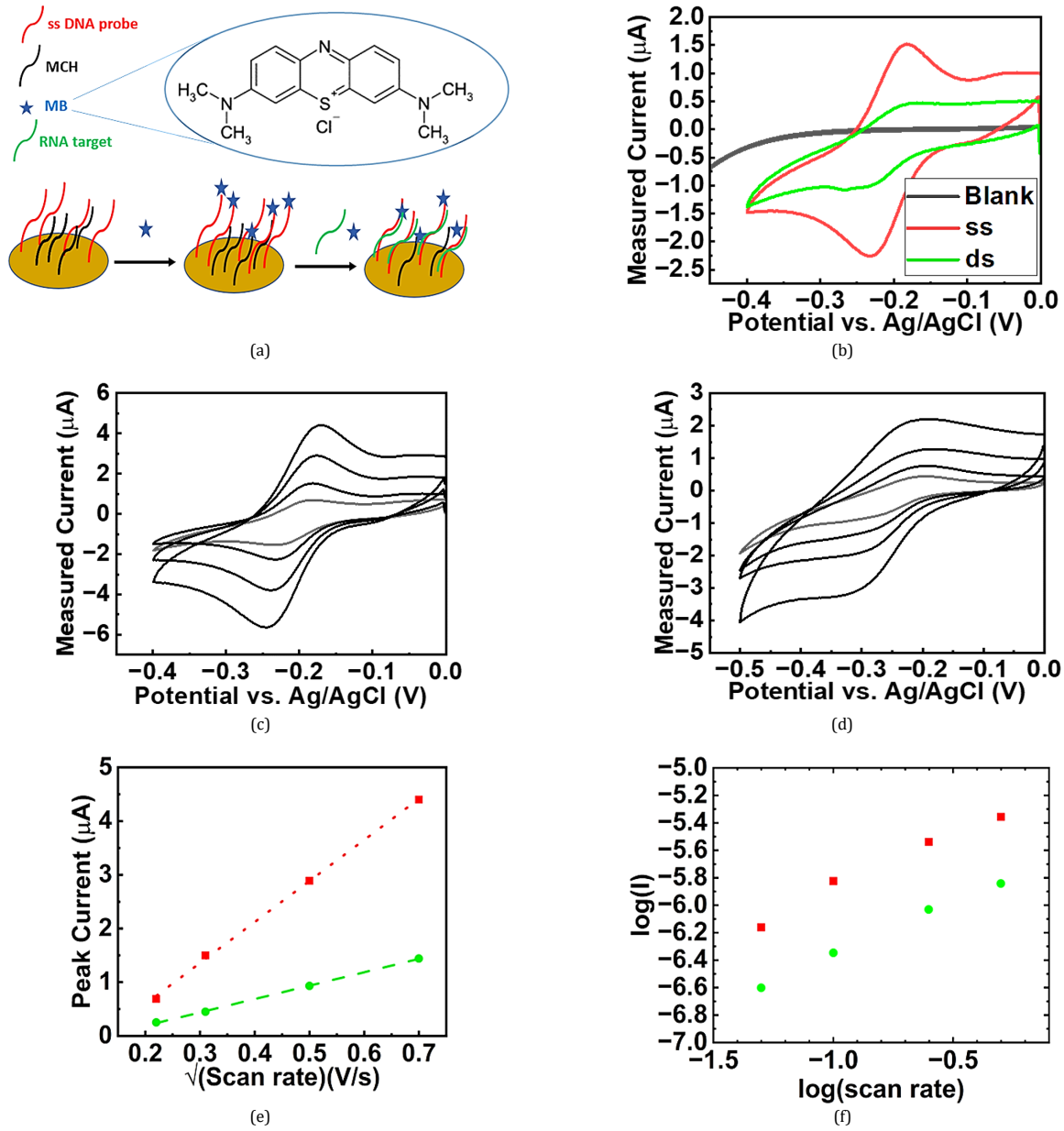

Figure 1. (A). Scheme of the self-assembled monolayers-modified electrodes. (B). Cyclic voltammograms (CV) of 20 μM methylene blue (MB) on ssDNA-MCH-Au (red) and ds (DNA:RNA)-MCH-Au (green). The black curve is a 'blank' CV measurement obtained with the ssDNA MCH-Au electrode prior to adding MB. Scan rate = 100 mV/s. (C) Scan rate dependence for the ssDNA-MCH-Au and (D) ds-MCH-Au. CVs collected with scan rates of 50, 100, 250, and 500 mV/s for both C and D (E) Plot of oxidative peak current *vs* scan rate$^{1/2}$ for ssDNA-MCH-Au (red) and ds-MCH-Au (green). The discontinuous lines are linear fits. (F) Log – log plot for current vs. scan rate.

To evaluate the effectiveness of the biosensor in terms of specificity, we compare the percentage of the oxidation peak signal reduction for the perfectly matched and the mismatched G12V DNA: RNA hybrids. Figure 2c presents a bar graph with the results. The bar graph shows that the signal reduction (%) for the perfect-match and mismatched hybrids has no significant difference. These results highlight an important limitation of this electrochemical biosensing strategy: its inability to differentiate the perfectly matched hybrid from the mismatched hybrid. More sophisticated approaches may be needed to detect single-base variations using electrochemistry [49]. This contrasts with the single-molecule electrical detection of the same biomarker [12,35], which offers the possibility of discriminating between sequences differing in a single base [12,50].

3.3. Sensitivity of the electrochemical approach for KRAS G12V detection (limit of detection)

To assess the sensitivity of the electrochemical approach to detect the KRAS G12V mutation, we perform titration experiments to determine the limit of detection (LOD) of the system using varying concentrations of KRAS G12V. Figure 2d presents the CVs obtained for the ssDNA probe and the 18-base pair KRAS G12V DNA:RNA hybrids, ranging from 4 zM (zeptomolar, 1×10^{-21} M) to 4 μM. The black curve represents the control experiment without the presence of MB or the RNA target (ssDNA-MCH Au). As shown in Figure 2d, the measured current decreases as the concentration of G12V RNA increases, compared to the signal of the ssDNA probe. In general, the LOD can be defined as the smallest concentration of an analyte that could be reliably measured by an analytical method [51,52].

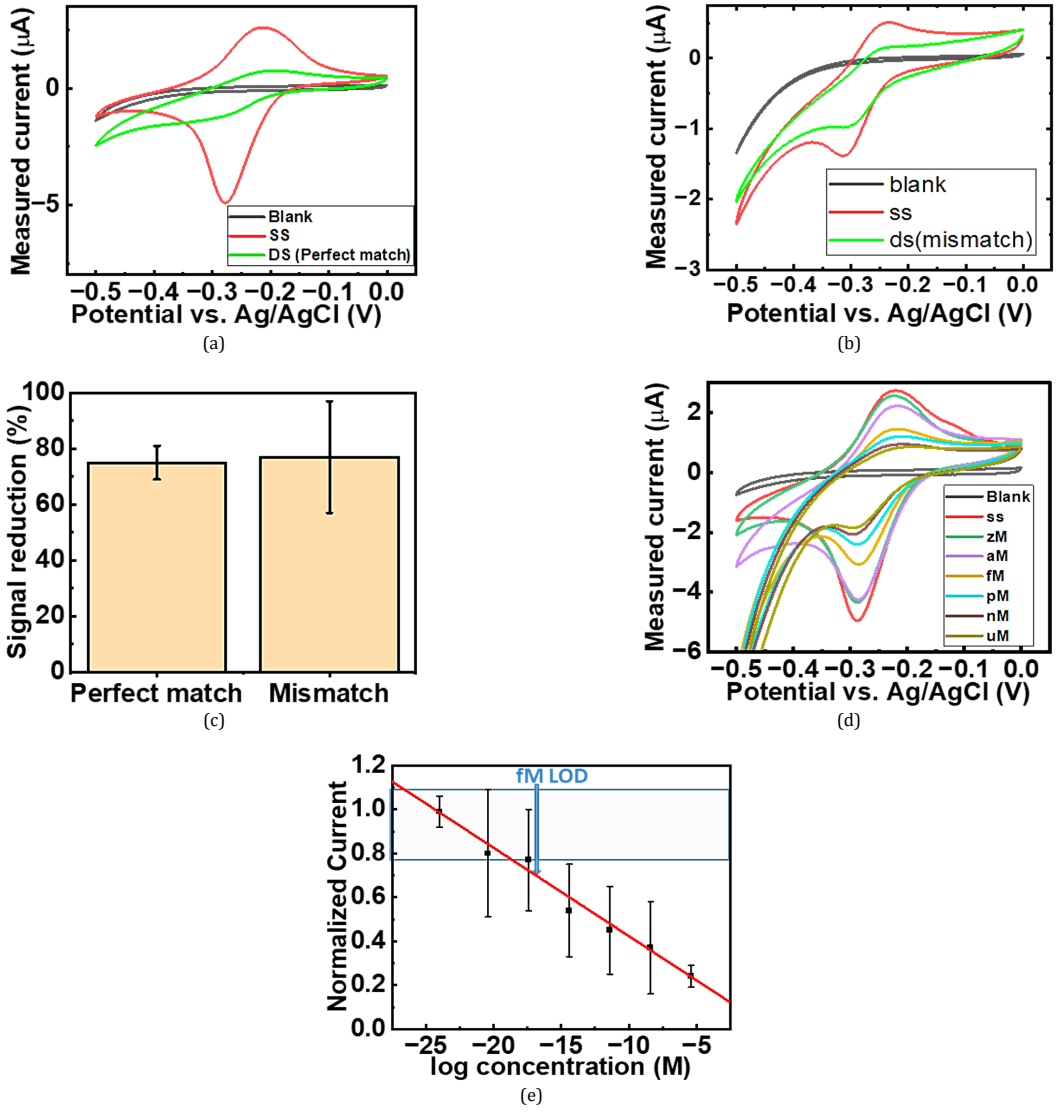

Figure 2. (a) CV for G12V perfectly matched DNA:RNA hybrids. (b) CV for mismatched G12V DNA:RNA hybrids. The red lines correspond to the DNA probe before hybridization, while the green lines are DNA:RNA hybrids. The black curves are a 'blank' CV measurements obtained with the ssDNA MCH-Au electrode prior to adding MB. (c) Bar chart of the oxidation peak signal reduction (%) for the G12V perfect match and mismatch hybrids compared to the ssDNA probe signal. The error bars are the standard deviation of three measurements. (d) CVs for G12V titration experiments at varying RNA concentration (from 4 μM to 4 zM). A control experiment (black, phosphate buffer) shows no oxidation or reduction peaks. (e) Plot of the normalized oxidation current of the titration experiments vs. the logarithmic concentration (M) of the RNA target. Each concentration was tested in three independent experiments at 100 mV/s (error bars are the standard error of the mean, n = 3).

In this case, we define the LOD as the target RNA concentration at which the RNA target signal can be detected with a statistical significance of three standard deviations away from the ssDNA probe background signal. Figure 2e illustrates a graph of the normalized current (oxidation peak) from the titration experiments against the logarithm of the RNA target concentration (M). Figure 2e shows that at the fM concentration level, one could distinguish the signal of the target RNA from the background. Furthermore, this fM level LOD aligns well with the LOD values reported in the literature for similar types of electrochemical biosensors [53-55]. These findings demonstrate the sensitivity of this traditional and relatively simple electrochemical approach to detect G12V RNA, allowing for RNA measurements even at low concentrations. It should be noted that this LOD is in agreement with previous research in the field [35,53-55].

3.4. Detection in complex media

To compare the selectivity of the electrochemical and STM-BJ approaches to detect KRAS G12V RNA, we also conduct a series of experiments in two distinct complex media: BSA (Bovine Serum Albumin) and calf-thymus DNA. BSA is a complex protein medium characterized by its tertiary globular structure and rich composition in α-helices [53]. Initially, we do CV experiments in a concentration of BSA medium with a 0.01 μg/mL. Figure 3A presents a representative example of such experiments in 0.01 μg/mL BSA medium, where we observe a decrease in the electrochemical signal upon hybridization with the complementary G12V RNA target. This decrease in signal shows the differentiation between the ssDNA probe background and the DNA:RNA hybridization signal, even in the presence of proteins. To further explore the performance of our electrochemistry approach, we conduct CV experiments with higher BSA concentrations of 10 μg/mL (Figure 4a) and 10 mg/mL (Figure 4b).

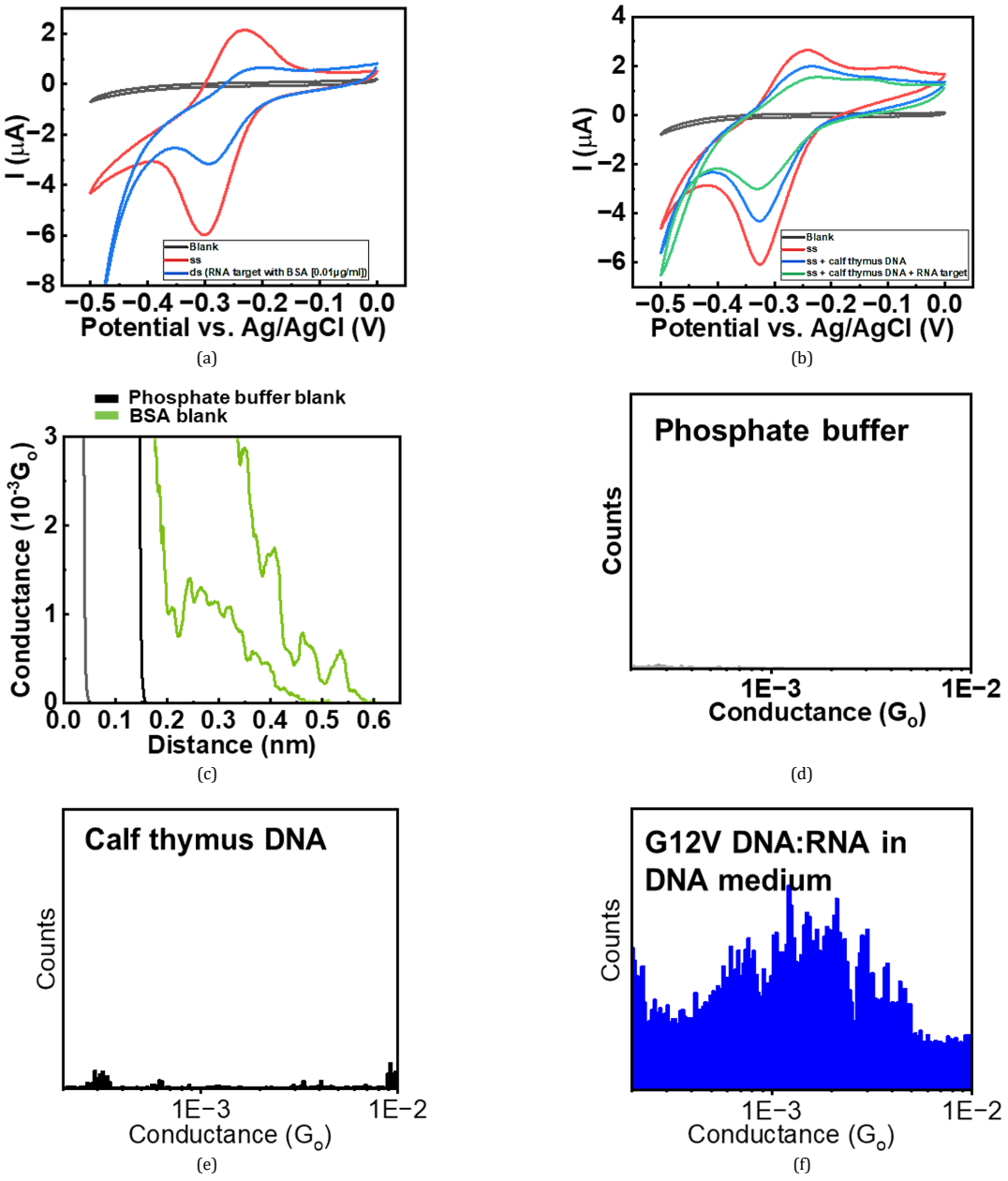

Figure 3. (A) CV experiment in a concentration of BSA medium with a 0.01 μg/mL (Black curve: Blank measurement, Red: ssDNA probe, Blue: DNA: RNA hybrids in 0.01 μg/mL BSA medium) (B) CV experiment in the presence of calf thymus DNA as background nucleic acid interference (black curve: Blank measurement, Red: ssDNA probe, Blue: ssDNA probe in calf-thymus DNA medium, Green: DNA:RNA hybrids in calf-thymus DNA medium) (C) Example raw data curves obtained from STM-BJ experiments in a phosphate buffer (black) and 10 μg/ml BSA media (green) (D) Conductance histogram for blank phosphate buffer (E) Conductance histogram for calf-thymus DNA blank experiments (F) Conductance histogram of G12V DNA:RNA in 0.9 ng/mL calf-thymus DNA. Single-molecule conductance expressed as G_0 (where $G_0=2e^2/h \approx 77.5$ μS).

The 10 mg/ml BSA concentration experiment (Figure 4b) did not produce results, as we could not observe a clear decrease in the signal. It is worth noting that the normal protein concentration in serum is reported to be in the range of 60-80 mg/mL [56]. While, in theory, we can detect G12V RNA targets at lower BSA concentrations using the electrochemical approach, it would not be practical for real liquid biopsies due to the likely high protein levels present in real samples. This could be solved by including preprocessing steps of the samples and/or diluting them to reach a lower protein concentration. Similarly, we evaluate the performance of our quantum transport-based RNA cancer biomarker electrical detection using STM-BJ [12], but in this case, within a complex BSA medium. To begin, we perform a blank STM-BJ experiment in buffer solution to assess the STM tip quality and stability, followed by another blank experiment in a medium with a BSA concentration of 10 μg/mL. Figure 3c shows raw data curve examples for these experiments. No distinct steps appear in the phosphate buffer blank, represented by the black curves in Figure 3c. However, we encounter noisier conductance curves in the BSA experiment (green curves in Figure 3c), and a clean BSA blank conductance histogram cannot be obtained. This confirms that the detection of nucleic acids within the complex BSA medium using the STM-BJ approach is highly challenging, if possible at all. For real-world sensing applications, one should also use preprocessing steps in this case to reduce the protein concentration or purify nucleic acids, as previously suggested [33].

Table 2. Performance comparison for some strategies for KRAS biomarkers detection.

KRAS mutation	Strategy	Limit of detection	Specificity and single-base discrimination / Detection range probed	Reference
G12C	Electrochemical current modulation via a methylene-blue redox reporter using probe DNA	fM	No / fM - mM	This work
G12C	Single-molecule STM-BJ conductance measurements	aM	Yes / aM - mM	[12,15] and this work
G12V	Allele-specific PCR preamplification with CRISPR-Cas13a fluorescence-based detection	N.A. / 0.5% Mutant Allele Frequency (G12D demonstrated, adaptable to G12V)	Point-mutation discrimination ratio 22.9±8.8/ DNA inputs of 6-10 ng	[63]
G12V	Amperometry coupled with RCA and LNA probes	61 pM	Yes / 0.5 nM - 10 nM	[64]
G12D	PCR coupled with T7 endonuclease-mediated voltammetry	11.89 fM	Yes / fM - µM	[65]
G12D	Anchor-like DNA electrochemical biosensor	0.10 pM	Yes / pM - nM	[66]
G12D	Nanocomposites-based toehold-mediated DNA strand displacement	0.38 fM	Yes / 10 fM -10 nM	[67]
G12C	Label-free impedance biosensor	86.9 fM	Not tested / 0.1 pM - 1 µM	[68]

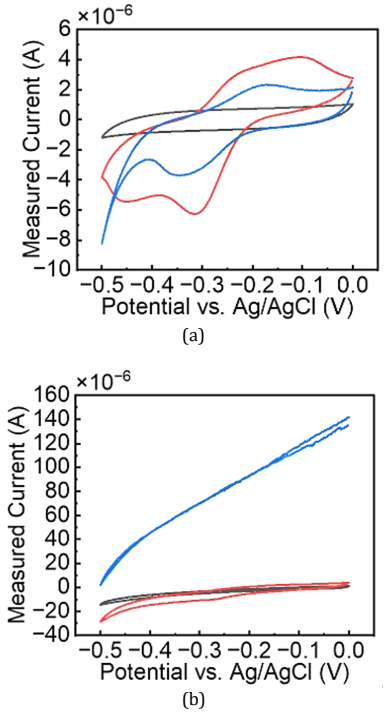

Figure 4. Experiments with different BSA concentrations. (a) CV in a BSA medium with a 10 µg/mL concentration. Black curve: phosphate buffer blank measurement, red: ssDNA sample, and blue: DNA:RNA hybrids, both in 10 µg/mL BSA medium (b) Example CV experiment in a 10 mg/mL BSA medium. Same color code as in A.

To further assess the selectivity of cancer biomarker detection in a complex medium, we conducted CV and STM-BJ experiments in the presence of cell-free DNA as a background interference medium. In this study, we mimic the presence of cell-free DNA by using commercial calf thymus DNA. As Figure 3b shows, we perform CV experiments starting from a blank measurement, followed by experiments involving the ssDNA probe alone, ssDNA probe in calf-thymus DNA medium, and finally adding the G12V RNA target. CV measurements for the ssDNA probe exhibit a higher signal compared to the blank measurement, indicating successful identification of the ssDNA probe. However, when calf thymus DNA (at a concentration of 0.9 ng/mL) is introduced alongside the ssDNA probe, a noticeable decrease in signal is observed. Calf thymus DNA acts as background interference and potentially hinders the diffusion of the MB toward the electrode surface. Similarly, when we measure the signal in the presence of both the G12V complementary RNA target and the interfering DNA, a further decrease in the signal is observed after hybridization. These findings suggest that obtaining a specific and discernible signal for the RNA biomarker becomes challenging in the presence of nucleic acids with this simple electrochemical scheme. This suggests that a completely new strategy may be necessary to detect cancer biomarkers with enough specificity and sensitivity using non-covalently bound MB electrochemical detection [41,57].

For comparison, we also performed STM-BJ experiments in the presence of calf thymus DNA as a background interference. As Figure 3d shows, we begin with a control experiment with phosphate buffer (pH = 7.4) that does not show a conductance peak. Next, we introduce calf-thymus DNA into the system at a concentration of 0.9 ng/mL. The conductance histogram obtained from this experiment shows a similar featureless profile similar to the phosphate buffer control (Figure 3e). The presence of calf-thymus DNA does not generate a discernible conductance peak, suggesting that it does not significantly affect conductance measurements in this context. To assess the selectivity of the detection method, we then introduce G12V perfect match DNA:RNA hybrids into the system along with the calf-thymus DNA. This addition results in a conductance peak observed at approximately 19.3×10^{-4} G_0 (where $G_0 = 2e^2/h \approx 77.5$ µS), in agreement with previously published results [12].

This demonstrates the successful detection of a cancer biomarker using the STM-BJ approach in a complex nucleic acid medium. However, it is essential to acknowledge that the concentration of cell-free DNA in real samples may vary [58-61]. Studies have reported that plasma samples from healthy individuals typically contain between 10 and 30 ng/ml of cell-free DNA [56]. Furthermore, the concentration of cell-free DNA in plasma has been found to be significantly higher in cancer patients compared to healthy subjects [59]. Moreover, the concentration of circulating tumor DNA (ctDNA) in mice bearing small tumors has been reported to range from 0.23 to 4.8 ng/mL [60]. These variations can be influenced by factors such as disease states or behavioral changes [58]. Therefore, when a biosensor to detect cancer biomarkers using electrical and electrochemical approaches, it is crucial to consider the potential variations in cell-free DNA or circulating tumor DNA concentrations and the underlying factors that can influence these levels. Understanding these aspects will enable the development of robust and reliable biosensing platforms that could effectively detect cancer biomarkers in real-world scenarios.

Table 2 summarizes the comparison of the performance of both biodetection methods. Both STM-BJ and electrochemical approaches have significant potential to advance cancer screening methodologies. The STM-BJ method offers attomolar sensitivity (aM) [12,15], enabling detection of cancer biomarkers at extremely low concentrations, and provides label-free detection with a demonstrated ability to identify single-base mismatches, even in the presence of interfering nucleic acids such as calf-thymus DNA [12,15,48]. On the contrary, the electrochemical approach is simple and cost-effective, making it suitable for large-scale screening, with a limit of detection in the femtomolar (fM) range [35,53]. However, its sensitivity and specificity for low-abundance biomarkers remain limited. Future strategies could focus on improving the detection capabilities of electrochemistry and overcoming these limitations. The potential for miniaturization of single-molecule biosensors also opens opportunities for point-of-care testing and remote disease monitoring [8]. A practical workflow might use the electrochemical sensor for rapid bulk screening, with positive samples subsequently analyzed by single-molecule readout for definitive mutation verification. Shared sample preparation steps, such as protein depletion and nucleic acid enrichment, could be used to streamline both stages, reduce the overall assay complexity, and potentially integrate into the initial electrochemical step [33,62].

4. Conclusions

In summary, we investigated an electrochemical approach for detecting the KRAS G12V RNA cancer biomarker and compared it with a single-molecule electrical detection method, including assessments in complex media. The electrochemical approach demonstrated lower sensitivity compared to the single-molecule biosensor. Both methods encountered challenges when applied in complex protein-rich media such as BSA. However, the STM-BJ approach was able to obtain conductance measurements for KRAS G12V biomarkers in the presence of complex DNA media, effectively distinguishing the hybrid signal from background interference. Some of the challenges may be addressed by integrating the two approaches into a two-tier purification and detection workflow, as previously demonstrated for *E. coli*. The use of the complementary strengths of both methods could enhance the detection of biomarkers in liquid biopsy applications.

Disclosure statement

Conflict of interest: The authors declare that they have no conflict of interest.
Ethical approval: All applicable ethical guidelines were followed.
Data availability: All processed data generated and analyzed during this study are included in this published article. Additional datasets are available from the corresponding author upon reasonable request.
Disclaimer: The views expressed in this article are solely those of the authors and do not necessarily reflect the official position of the ERCEA or the European Commission.

CRediT authorship contribution statement

Conceptualization: Juan Manuel Artés Vivancos Methodology: Ajoke Williams, Keshani G Gunasinghe Pattiya Arachchillage Writing - Ajoke Williams, Keshani G Gunasinghe Pattiya Arachchillage, Juan Manuel Artés Vivancos Writing - Review and Editing: Ajoke Williams, Keshani G Gunasinghe Pattiya Arachchillage, Subrata Chandra, Juan Manuel Artés Vivancos. Supervision: Juan Manuel Artés Vivancos.

ORCID and Email

Ajoke Williams
ajoke_williams@student.uml.edu
https://orcid.org/0000-0001-5314-0590
Keshani Gayathri Gunasinghe Pattiya Arachchillage
keshani_pattiyaarachchillage@student.uml.edu
https://orcid.org/0000-0002-5118-7018
Subrata Chandra
subrata_chandra@student.uml.edu
https://orcid.org/0009-0001-5012-9684
Juan Manuel Artés Vivancos
juan.artes-vivancos@ec.europa.eu
https://orcid.org/0000-0002-5050-3760

References

[1]. Wadgaonkar, P. Environmental causes of cancer. *Cancer Epigenetics Nanomedicine* **2024**, 69–92.
[2]. Bhat, G. R.; Sethi, I.; Sadida, H. Q.; Rah, B.; Mir, R.; Algehainy, N.; Albalawi, I. A.; Masoodi, T.; Subbaraj, G. K.; Jamal, F.; Singh, M.; Kumar, R.; Macha, M. A.; Uddin, S.; Akil, A. S.; Haris, M.; Bhat, A. A. Cancer cell plasticity: from cellular, molecular, and genetic mechanisms to tumor heterogeneity and drug resistance. *Cancer Metastasis. Rev.* **2024**, *43* (1), 197–228.
[3]. Cancer statistics. https://www.cancer.gov/about-cancer/understanding/statistics (accessed Feb 10, 2026).
[4]. Cancer. https://www.who.int/news-room/fact-sheets/detail/cancer (accessed Feb 10, 2026).
[5]. Mikaeeli Kangarshahi, B.; Naghib, S. M.; Rabiee, N. DNA/RNA-based electrochemical nanobiosensors for early detection of cancers. *Critical Rev. Clin. Lab. Sci.* **2024**, *61* (6), 473–495.
[6]. Bengtsson, A.; Andersson, R.; Ansari, D. The actual 5-year survivors of pancreatic ductal adenocarcinoma based on real-world data. *Sci. Rep.* **2020**, *10* (1), 16425 https://doi.org/10.1038/s41598-020-73525-y.
[7]. Wang, H.; Liu, J.; Xia, G.; Lei, S.; Huang, X.; Huang, X. Survival of pancreatic cancer patients is negatively correlated with age at diagnosis: a population-based retrospective study. *Sci. Rep.* **2020**, *10* (1), 7048 https://doi.org/10.1038/s41598-020-64068-3.
[8]. Williams, A.; Aguilar, M. R.; Pattiya Arachchillage, K. G.; Chandra, S.; Rangan, S.; Ghosal Gupta, S.; Artes Vivancos, J. M. Biosensors for Public Health and Environmental Monitoring: The Case for Sustainable Biosensing. *ACS Sustainable Chem. Eng.* **2024**, *12* (28), 10296–10312.
[9]. Zhu, L.; Zhao, R.; Wang, K.; Xiang, H.; Shang, Z.; Sun, W. Electrochemical Behaviors of Methylene Blue on DNA Modified Electrode and Its Application to the Detection of PCR Product from NOS Sequence. *Sensors* **2008**, *8* (9), 5649–5660.
[10]. Drummond, T. G.; Hill, M. G.; Barton, J. K. Electrochemical DNA sensors. *Nat. Biotechnol.* **2003**, *21* (10), 1192–1199.
[11]. Kerman, K.; Ozkan, D.; Kara, P.; Meric, B.; Gooding, J. J.; Ozsoz, M. Voltammetric determination of DNA hybridization using methylene blue and self-assembled alkanethiol monolayer on gold electrodes. *Anal. Chim. Acta* **2002**, *462*, 39–47.
[12]. Pattiya Arachchillage, K. G.; Chandra, S.; Williams, A.; Piscitelli, P.; Pham, J.; Castillo, A.; Florence, L.; Rangan, S.; Artes Vivancos, J. M. Electrical detection of RNA cancer biomarkers at the single-molecule level. *Sci. Rep.* **2023**, *13* (1), https://doi.org/10.1038/s41598-023-39450-6.

[13]. Gunasinghe Pattiya Arachchillage, K. G.; Chandra, S.; Williams, A.; Rangan, S.; Piscitelli, P.; Florence, L.; Ghosal Gupta, S.; Artes Vivancos, J. M. A single-molecule RNA electrical biosensor for COVID-19. *Biosensors Bioelectronics* **2023**, *239*, 115624.

[14]. Wu, Y.; Arroyo-Currás, N. Advances in nucleic acid architectures for electrochemical sensing. *Current Opinion Electrochem.* **2021**, *27*, 100695.

[15]. Li, Y.; Artés, J. M.; Demir, B.; Gokce, S.; Mohammad, H. M.; Alangari, M.; Anantram, M. P.; Oren, E. E.; Hihath, J. Detection and identification of genetic material via single-molecule conductance. *Nature Nanotech.* **2018**, *13* (12), 1167–1173.

[16]. Chandra, S.; Williams, A.; Maksudov, F.; Kliuchnikov, E.; Pattiya Arachchillage, K. G.; Piscitelli, P.; Castillo, A.; Marx, K. A.; Barsegov, V.; Artes Vivancos, J. M. Charge transport in individual short base stacked single-stranded RNA molecules. *Sci. Rep.* **2023**, *13* (1), 19858 https://doi.org/10.1038/s41598-023-46263-0.

[17]. Chandra, S.; Gunasinghe Pattiya Arachchillage, K. G.; Kliuchnikov, E.; Maksudov, F.; Ayoub, S.; Barsegov, V.; Artés Vivancos, J. M. Single-molecule conductance of double-stranded RNA oligonucleotides. *Nanoscale* **2022**, *14* (7), 2572–2577.

[18]. Gu, C.; Jia, C.; Guo, X. Single-Molecule Electrical Detection with Real-Time Label-Free Capability and Ultrasensitivity. *Small. Methods.* **2017**, *1* (5), 1700071 https://doi.org/10.1002/smtd.201700071.

[19]. Dief, E. M.; Low, P. J.; Díez-Pérez, I.; Darwish, N. Advances in single-molecule junctions as tools for chemical and biochemical analysis. *Nat. Chem.* **2023**, *15* (5), 600–614.

[20]. Labib, M.; Sargent, E. H.; Kelley, S. O. Electrochemical Methods for the Analysis of Clinically Relevant Biomolecules. *Chem. Rev.* **2016**, *116* (16), 9001–9090.

[21]. Boal, A. K.; Barton, J. K. Electrochemical Detection of Lesions in DNA. *Bioconjugate Chem.* **2005**, *16* (2), 312–321.

[22]. Sfragano, P. S.; Pillozzi, S.; Palchetti, I. Electrochemical and PEC platforms for miRNA and other epigenetic markers of cancer diseases: Recent updates. *Electrochem. Commun.* **2021**, *124*, 106929.

[23]. Ju, H.-X.; Ye, Y.-K.; Zhao, J.-H.; Zhu, Y.-L. Hybridization biosensor using di(2,2'-bipyridine)osmium (III) as electrochemical indicator for detection of polymerase chain reaction product of hepatitis B virus DNA. *Anal. Biochem.* **2003**, *313*, 255–261.

[24]. Wang, J.; Chicharro, M.; Rivas, G.; Cai, X.; Dontha, N.; Farias, P. A.; Shiraishi, H. DNA Biosensor for the Detection of Hydrazines. *Anal. Chem.* **1996**, *68* (13), 2251–2254.

[25]. Xu, X.-H.; Bard, A. J. Immobilization and hybridization of DNA on an aluminum(III) alkanebisphosphonate thin film with electrogenerated chemiluminescent detection. *J. Am. Chem. Soc.* **1995**, *117*, 2627–2631.

[26]. Jiao, K.; Xu, G.; Zhang, X.; Mi, C. Preparation and voltammetric characterization of DNA modified electrode with ethylenediamine as arm molecule. *Gaodeng Xuexiao Huaxue Xuebao / Chemical Journal of Chinese Universities-Chinese* **2005**, *26* (5), 841-843.

[27]. Millan, K. M.; Saraullo, A.; Mikkelsen, S. R. Voltammetric DNA Biosensor for Cystic Fibrosis Based on a Modified Carbon Paste Electrode. *Anal. Chem.* **1994**, *66* (18), 2943–2948.

[28]. Tokonami, S.; Shiigi, H.; Nagaoka, T. Preparation of Nanogapped Gold Nanoparticle Array for DNA Detection. *Electroanalysis* **2008**, *20* (4), 355–360.

[29]. Wang, M.; Sun, C.; Wang, L.; Ji, X.; Bai, Y.; Li, T.; Li, J. Electrochemical detection of DNA immobilized on gold colloid particles modified self-assembled monolayer electrode with silver nanoparticle label. *J. Pharm. Biomed. Anal.* **2003**, *33*, 1117–1125.

[30]. Wang, B.; Du, X.; Zheng, J.; Jin, B. Electrochemical sensor based on immobilization of single stranded deoxyribonucleic acid on Pt electrode surface by avidin-biotin system. *Chinese Journal of Analytical Chemistry* **2005**, *33* (6), 789-792.

[31]. Lucarelli, F.; Marrazza, G.; Turner, A. P. F.; Mascini, M. Carbon and gold electrodes as electrochemical transducers for DNA hybridisation sensors. *Biosens. Bioelectron.* **2004**, *19*, 515–530.

[32]. Lord, H.; Kelley, S. O. Nanomaterials for ultrasensitive electrochemical nucleic acids biosensing. *J. Mater. Chem.* **2009**, *19* (20), 3127–3134.

[33]. Veselinovic, J.; Alangari, M.; Li, Y.; Matharu, Z.; Artés, J. M.; Seker, E.; Hihath, J. Two-tiered electrical detection, purification, and identification of nucleic acids in complex media. *Electrochim. Acta* **2019**, *313*, 116–121.

[34]. Kelley, S. O.; Barton, J. K.; Jackson, N. M.; Hill, M. G. Electrochemistry of Methylene Blue Bound to a DNA-Modified Electrode. *Bioconjugate. Chem.* **1997**, *8* (1), 31–37.

[35]. Pattiya Arachchillage, K. G.; Chandra, S.; Piso, A.; Qattan, T.; Artes Vivancos, J. M. RNA BioMolecular Electronics: towards new tools for biophysics and biomedicine. *J. Mater. Chem. B* **2021**, *9* (35), 6994–7006.

[36]. Chandra, Subrata. "Physicochemical Investigation and Electrical Measurement of Biomolecular Interactions at the Single-Molecule Level." Order No. 30569148 University of Massachusetts Lowell, 2023. United States -- Massachusetts: ProQuest. Web. 8 Feb. 2026.

[37]. Pattiya Arachchillage, Keshani G. Gunasinghe. "Single-Molecule RNA Electrical Detection for Applications in Cancer and COVID-19." Order No. 30566679 University of Massachusetts Lowell, 2023. United States -- Massachusetts: ProQuest. Web. 8 Feb. 2026.

[38]. Aguilar, M. R.; Jover, J.; Ruiz, E.; Aragonès, A. C.; Artés Vivancos, J. M. Single-Molecule Electrical Conductance in Z-form DNA:RNA. *Small.* **2024**, *21* (5), 2408459 https://doi.org/10.1002/smll.202408459.

[39]. Disulfide reduction using TCEP reaction. https://www.biosyn.com/tew/instruction-of-reduction-reaction-using-tcep.aspx (accessed Feb 10, 2026).

[40]. Hihath, J.; Tao, N. Rapid measurement of single-molecule conductance. *Nanotechnology* **2008**, *19* (26), 265204.

[41]. Pheeney, C. G.; Barton, J. K. DNA Electrochemistry with Tethered Methylene Blue. *Langmuir* **2012**, *28* (17), 7063–7070.

[42]. Herne, T. M.; Tarlov, M. J. Characterization of DNA Probes Immobilized on Gold Surfaces. *J. Am. Chem. Soc.* **1997**, *119* (38), 8916–8920.

[43]. Yang, W.; Ozsoz, M.; Hibbert, D. B.; Gooding, J. J. Evidence for the direct interaction between methylene blue and guanine bases using DNA-modified carbon paste electrodes. *Electroanalysis* **2002**, *14*, 1299–1302.

[44]. Bard, A. J.; Faulkner, L. R.; White, H. S. Electrochemical methods: fundamentals and applications; John Wiley & Sons, 2022.

[45]. Haque, F.; Rahman, M.; Ahmed, E.; Bakshi, P.; Shaikh, A. A Cyclic Voltammetric Study of the Redox Reaction of Cu(II) in Presence of Ascorbic Acid in Different pH Media. *Dhaka. Univ. J. Sci.* **2013**, *61* (2), 161–166.

[46]. Evans, D. H.; O'Connell, K. M.; Petersen, R. A.; Kelly, M. J. Cyclic voltammetry. *J. Chem. Educ.* **1983**, *60* (4), 290.

[47]. García-González, R.; Costa-García, A.; Fernández-Abedul, M. T. Methylene blue covalently attached to single stranded DNA as electroactive label for potential bioassays. *Sensors Actuators B: Chem.* **2014**, *191*, 784–790.

[48]. Batchelor, R. H.; Dief, E. M.; Bonham, A. J.; Gooding, J. J. A Review of Methylene Blue's Interactions with DNA and Their Relevance for DNA-Based Sensors. *ACS. Sens.* **2025**, *10* (6), 3854–3877.

[49]. Li, H.; Arroyo-Currás, N.; Kang, D.; Ricci, F.; Plaxco, K. W. Dual-Reporter Drift Correction To Enhance the Performance of Electrochemical Aptamer-Based Sensors in Whole Blood. *J. Am. Chem. Soc.* **2016**, *138* (49), 15809–15812.

[50]. Hihath, J.; Xu, B.; Zhang, P.; Tao, N. Study of single-nucleotide polymorphisms by means of electrical conductance measurements. *Proc. Natl. Acad. Sci. U.S.A.* **2005**, *102* (47), 16979–16983.

[51]. Rousseau, R. M. Detection limit and estimate of uncertainty of analytical XRF results. *Rigaku J.* **2001**, *18* (2), 33–47.

[52]. Armbruster, D. A.; Pry, T. Limit of blank, limit of detection and limit of quantitation. *Clin. Biochem. Rev.* **2008**, 29, S49–S52.

[53]. Sun, C.; Huang, H.; Wang, J.; Liu, W.; Yang, Z.; Yu, X. Applications of electrochemical biosensors based on 2D materials and their hybrid composites in hematological malignancies diagnosis. *Technol. Cancer. Res. Treat.* **2022**, *21*, https://doi.org/10.1177/15330338221142996.

[54]. Spring, S. A.; Goggins, S.; Frost, C. G. Ratiometric Electrochemistry: Improving the Robustness, Reproducibility and Reliability of Biosensors. *Molecules.* **2021**, *26* (8), 2130.

[55]. Terzapulo, X.; Dyussupova, A.; Ilyas, A.; Boranova, A.; Shevchenko, Y.; Mergenbayeva, S.; Filchakova, O.; Gaipov, A.; Bukasov, R. Detection of Cancer Biomarkers: Review of Methods and Applications Reported from Analytical Perspective. *Crit. Rev. Anal. Chem.* **2025**, 1–46.

[56]. Busher, J. T. Serum Albumin and Globulin. In Clinical Methods: The History, Physical, and Laboratory Examinations; Walker, H. K.; Hall, W. D.; Hurst, J. W., Eds. In: Clinical Methods: The History, Physical, and Laboratory Examinations. 3rd edition. Boston: Butterworths; 1990. Chapter 101.

[57]. Furst, A. L.; Hill, M. G.; Barton, J. K. Electrocatalysis in DNA sensors. *Polyhedron* **2014**, *84*, 150–159.

[58]. Quinones, I.; Daniel, B. Cell free DNA as a component of forensic evidence recovered from touched surfaces. *Forensic. Science. Inter. Genetics* **2012**, *6* (1), 26–30.

[59]. Alborelli, I.; Generali, D.; Jermann, P.; Cappelletti, M. R.; Ferrero, G.; Scaggiante, B.; Bortul, M.; Zanconati, F.; Nicolet, S.; Haegele, J.; Bubendorf, L.; Aceto, N.; Scaltriti, M.; Mucci, G.; Quagliata, L.; Novelli, G. Cell-free DNA analysis in healthy individuals by next-generation sequencing: a proof of concept and technical validation study. *Cell. Death. Dis.* **2019**, *10* (7), https://doi.org/10.1038/s41419-019-1770-3.

[60]. Mouliere, F.; Robert, B.; Arnau Peyrotte, E.; Del Rio, M.; Ychou, M.; Molina, F.; Gongora, C.; Thierry, A. R. High Fragmentation Characterizes Tumour-Derived Circulating DNA. *PLoS ONE* **2011**, *6* (9), e23418.

[61]. Song, P.; Wu, L. R.; Yan, Y. H.; Zhang, J. X.; Chu, T.; Kwong, L. N.; Patel, A. A.; Zhang, D. Y. Limitations and opportunities of technologies for the analysis of cell-free DNA in cancer diagnostics. *Nat. Biomed. Eng.* **2022**, *6* (3), 232–245.

[62]. Gu, Q.; Petrek, Z.; Rezayan, R.; Ye, T. Single molecule insights into interfacial molecular recognition for model electrochemical DNA biosensors. *Current Opinion Electrochem.* **2023**, *40*, 101348.

[63]. Amintas, S.; Cullot, G.; Boubaddi, M.; Rébillard, J.; Karembe, L.; Turcq, B.; Prouzet-Mauléon, V.; Bedel, A.; Moreau-Gaudry, F.; Cappellen, D.;

Dabernat, S. Integrating allele-specific PCR with CRISPR-Cas13a for sensitive KRAS mutation detection in pancreatic cancer. *J. Biol. Eng.* **2024**, *18* (1), https://doi.org/10.1186/s13036-024-00450-3.
[64]. Sebuyoya, R.; Sevcikova, S.; Yusuf, B.; Bartosik, M. Integrating isothermal amplification techniques and LNA-based AI-assisted electrochemical bioassay for analysis of KRAS G12V point mutation. *Talanta.* **2025**, *288*, 127709.
[65]. Chowdhury, P.; Cha, B. S.; Kim, S.; Lee, E. S.; Yoon, T.; Woo, J.; Park, K. S. T7 Endonuclease I-mediated voltammetric detection of KRAS mutation coupled with horseradish peroxidase for signal amplification. *Microchim. Acta* **2022**, *189* (2), https://doi.org/10.1007/s00604-021-05089-1.
[66]. Zeng, N.; Xiang, J. Detection of KRAS G12D point mutation level by anchor-like DNA electrochemical biosensor. *Talanta* **2019**, *198*, 111–117.
[67]. Yu, X.; Bai, S.; Wang, L. In situ reduction of gold nanoparticles-decorated MXenes-based electrochemical sensing platform for KRAS gene detection. *Front. Bioeng. Biotechnol.* **2023**, *11*, https://doi.org/10.3389/fbioe.2023.1176046.
[68]. Zhang, Y.; Wei, H.; Guo, L.; Gao, W.; Cheng, D.; Liu, Y. A novel label-free impedance biosensor for KRAS G12C mutations detection based on PET-RAFT and ROP synergistic signal amplification. *Bioelectrochem.* **2025**, *161*, 108844.